Ceramics International 48 (2022) 18530–18540

Contents lists available at ScienceDirect

Ceramics International

journal homepage: www.elsevier.com/locate/ceramint

A micromechanical damage model for oxide/oxide ceramic matrix composites with hierarchical porosity under thermomechanical loading

Zheng-Mao Yang [a,*], Han Yan [b], Jun-Jie Yang [d], Xiao Li [c,**]

[a] Institute of Mechanics, Chinese Academy of Sciences, Beijing, 100190, China
[b] School of Aerospace Engineering, Tsinghua University, Beijing, 100084, China
[c] Beijing Spacecrafts, China Academy of Space Technology, Beijing, 100094, China
[d] Institute for Aero Engine, Tsinghua University, Beijing, 100084, China

ARTICLE INFO

Keywords:
Ceramic matrix composites
Hierarchical porosity
Micromechanical damage
Thermomechanical behaviors

ABSTRACT

This work presents a micromechanical damage model to describe the microstructural damage behaviors of ceramic matrix composites with hierarchical porosity during thermomechanical loading. The microstructure evolution may cause the nonlinear constitutive behavior, and a hierarchical porosity-based elasto-plastic constitutive model was developed. Damage mechanisms of matrix-crack, hierarchical pore nucleation and fiber-breaking are incorporated into the formulation of the damage model to describe various micromechanical damage modes of ceramic matrix composites accurately. Two damage variables are proposed for the damage evolution of matrix and fiber bundles. The main damage mechanisms in the matrix are matrix-cracking, and fibers breaking in the fiber bundles. The performance of the proposed damage model is verified by comparing with the existing experimental data. The proposed damage model outperforms the existing counterparts by capturing the microstructural damage mechanism and integrated into the damage model, and the contribution of different damage mechanisms can be quantified. The present work will provide a robust tool for describing the damage behaviors of matrix and fiber bundles in the ceramic matrix composites under thermomechanical loading, as well as allow a more accurate characterization of microstructural damage for a large extent of ceramic matrix composites.

1. Introduction

Ceramic matrix composites (CMCs), owning excellent design flexibility, high stiffness to weight ratio and high strength, are widely used in numerous structural components of aero-space applications [1,2]. However, accurate predictions of damage evolution for CMCs suffering from thermomechanical loading involve many, yet unsolved, challenges. Under thermomechanical loading, the thermal stress in the material leads to different microstructural damage types, such as hierarchical pore nucleation, microcracks and fiber breaking, all of which will produce substantially different effects on the overall mechanical properties of materials [3]. Although these damage scenarios improve the understanding of the behavior of CMCs, hierarchical porosity related to the manufacturing process is relatively rarely taken into account. This lack of knowledge of the influence of microstructural damage on mechanical behavior is the main motivation for the present study.

Accurately modeling the complex damage behaviors of CMCs under thermomechanical loading is a challenging work which limits the understanding of CMCs performance seriously. Salekeen et al. [4] used water quenching method to evaluate the thermal impact resistance of SiC-CMCs, and determined that the main damage mode under thermomechanical loading is matrix cracking. Kastritseas et al. [5] proposed the initiation criterion of multiple cracks in matrix considering the anisotropic stress field of CMCs under thermomechanical loading. A key objective in modeling the complex damage behaviors of CMCs is to capture the dominant damage mechanisms in the different components, as well as describe the propagation process of microstructural damage, so that the structural damage can be accurately predicted. In general, the damage forms in the CMCs including matrix cracks, nucleation and growth of pores, fiber-matrix interfacial debonding, fiber breaks, etc. Moreover, the presence of hierarchical porosity in the original material introduces additional complexities in describing the behaviors of

* Corresponding author.
** Corresponding author.
E-mail addresses: zmyang@imech.ac.cn (Z.-M. Yang), laughli1985@126.com (X. Li).

https://doi.org/10.1016/j.ceramint.2022.03.123
Received 17 December 2021; Received in revised form 12 March 2022; Accepted 12 March 2022
Available online 23 March 2022

materials. Therefore, the complex damage mechanisms motivate the need for a micromechanical damage model that integrates microstructural damage with specific composite components.

Recently, numerous research has been devoting to using micromechanics analysis methods to understand material behavior, some researchers paid attention to the microstructure of composites when considering the micromechanical models. Shen et al. [6,7] investigated a porous matrix including two populations of pores, and developed a two-step homogenization process for the pores to establish a micro-macro model, so that the elastoplastic behaviors of materials can be well described. The detailed research above has increased the understanding of the properties for CMCs, and these works are instrumental in establishing the micromechanical damage model for CMCs with hierarchical porosity. Considering the thermodynamics of the damage in the porous medium material, the continuum damage mechanics (CDM) and internal state variable (ISV) theory have been extensively used to derive damage laws. Shojaei et al. [8] developed a constitutive model based on the CDM to represent the damage behaviors of porous rocks considering the micro-void and microcrack fracture mechanics, the elastic-plastic behaviors were also included. Choi et al. [9] developed a mixing-unmixing model for porous woven composites to predict the property of materials, and the micro-state correction factors, as well as the poroelastic strain, were included in the thermoelastic constitutive equations. Nguyen et al. [10] developed constitutive models by defining the internal variables, which can be used to describe the micromechanical failure of materials, and macro and micro scale were involved in the localized failure mechanisms. Chen et al. [11] observed the behaviors of non-woven materials under uniaxial tensile loading, and established a micromechanical-based damage model to reproduce the experimental results. Skinner et al. [12] established a multiscale damage model for porous composites using the internal state variable theory, the growth and nucleation of matrix porosity, as well as matrix cracking, were taken into consideration in the damage model. However, the present listed models involve two limitations: They lack a mechanism for the complex damage behaviors in the fiber bundles and matrix of porous composites, as well as a consideration of the effects of hierarchical porosity on the material property. The primary objective of this work is to investigate these issues and try to develop an approach to deal with these problems.

In the present work, considering the effects of hierarchical porosity, a micromechanical damage model is established to describe the different damage behaviors of fiber bundles and matrix in CMCs under thermomechanical loading. Then different types of damage-micropores and microcracks for matrix and fiber bundles are discussed by defining damage variables. Besides, the elastic-plastic properties of CMCs are determined by proposed a constitutive law with hierarchical porosity. Finally, the soundness of the proposed damage model can be evaluated referring to experimental results by applying the model to a typical CMC. The benefits of the proposed model are that: (i) it provides a more sound prediction for the damage evolution in the fiber bundles and matrix of CMCs, as well as the overall material property when suffering from thermomechanical loading, and (ii) it captures the decrease of the property of fiber bundles and matrix due to the presence of the hierarchical porosity, the nucleation of pores as well as microcracks.

2. Material

In the present work, the tested material 2-D woven oxide/oxide CMCs consist of woven Nextel™ 610 fibers (99% α-Al_2O_3), which are embedded in a $Al_2O_3 - SiO_2 - ZrO_2$ matrix with a density of 4.2 g/cm^3. The uncoated Nextel™ 610 fibers with a density of 4.0 g/cm^3 are in 0°/90° woven layers. The fiber volume fraction of the CMCs is approximately 44%, and the matrix contains chemical compositions of 85% Al_2O_3 and 15% 3YSZ (in weight). The composites were produced using fabric type woven as 8 harness satin weave (HSW). The textile structures were impregnated with the paste-like Al_2O_3 slurry by knife blade coating. 12 layers were then stacked together, pressed and dried at 80 °C ~150 °C, the subsequent sintering process was conducted at 1100 °C ~1300 °C, followed by infiltration with a 3YSZ-sol and a second sintering process at the same temperature for 5 h.

2.1. Hierarchical porosity in oxide/oxide CMCs

Fig. 1 presents observations using a SEM of an oxide/oxide CMCs produced from a woven reinforcement of Nextel™ 610 fibers (alumina) and a aluminum matrix. In the 8 HSW preform, the fiber strands are oriented at 0°/90° and the matrix is porous. It is noted in these sectional views that the matrix has well infiltrated the strands of fibers and that the fibers are distributed in a dense and fairly homogeneous manner, which is necessary for the composite to have good mechanical properties. Views at lower magnifications reveal the presence of macropores, which correspond to air bubbles and which are linked to the molding process during processing. These voids appear at the intersection of the folds. SEM micrographs reveal a thin layer of matrix between the different plies of the laminate which contribute to obtaining a large volume fraction of fibers. On these composites, after processing, one can also observe a more or less regular matrix crack pattern, which is characteristic of the majority of oxide/oxide CMCs. These cracks appear due to differential shrinkage between the fibrous reinforcement and the matrix during sintering and are concentrated in areas rich in matrix.

Due to the specific manufacturing process of CMCs, there are many shrinkage cracks, intra-wire porosities and macroporosities inside the original material. Besides, the pores in the composite materials have obvious stratification characteristics both in the fiber bundles and matrix. Therefore, to describe the different sizes of pores, the concept of 'hierarchical porosity' was proposed in the previous work [13]. Fig. 1 shows the hierarchical porosity observation of a typical CMCs, and the material will be applied to the experimental validation later. There are two types of pores presents in the fiber bundles and matrix of material: (i) The nanopores, the diameter of which is a few nanometers, and they exist in the matrix around the particles, which are formed in the manufacturing process; (ii) The micropores, with a few microns in diameter, usually appear in the fiber bundles, matrix and interface. Micropores in the matrix have two patterns of manifestation, one is the sintering shrinkage cracks, and they are perpendicular to the plies, the other is air-filled cavities at the interface of matrix and fiber bundles. Micropores in the fiber bundles usually around fibers and caused by the lack of matrix.

Consider the volume of a composite is V, and the volume of nanopores is w_{I}, w_{II} is the volume of micropores, then,

$$\zeta_{\mathrm{I}} = \frac{|w_{\mathrm{I}}|}{|V|}, \quad \zeta_{\mathrm{II}} = \frac{|w_{\mathrm{II}}|}{|V|}, \quad \zeta = \frac{|w_{\mathrm{I}}| + |w_{\mathrm{II}}|}{|V|} = \zeta_{\mathrm{I}} + \zeta_{\mathrm{II}} \tag{1}$$

where ζ_{I} is the nanoporosity and ζ_{II} is the microporosity, ζ is the total porosity of the material. Besides, taking into account the observation of material, there are different distributions for hierarchical porosity in the fiber bundles and matrix, thus, it is necessary to investigate the porosity in the fiber bundles and matrix separately. The micropores appear both in the fiber bundles and matrix, while the nanopores only in the matrix. Therefore, the porosity of fiber bundles and matrix can be determined as,

$$\zeta_{\mathrm{f}} = \zeta_{\mathrm{II}}^{\mathrm{f}}, \quad \zeta_{\mathrm{m}} = \zeta_{\mathrm{I}} + \zeta_{\mathrm{II}}^{\mathrm{m}} \tag{2}$$

where $\zeta_{\mathrm{II}} = \zeta_{\mathrm{II}}^{\mathrm{f}} + \zeta_{\mathrm{II}}^{\mathrm{m}}$. Then the influence of hierarchical porosity on the property of matrix and fiber bundles can be investigated detailedly by using Eq. (2).

2.2. Microstructure evolution during thermomechanical loading

During the thermomechanical loading, the mechanical properties of CMCs will decrease due to the microstructural changes. Accurately

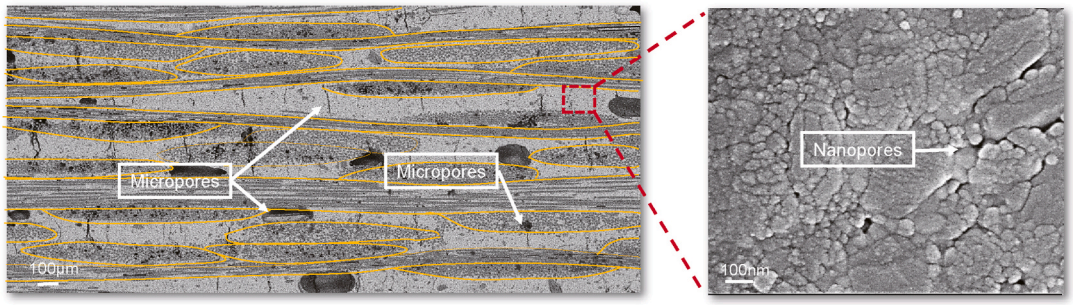

Fig. 1. Hierarchical porosity observation of a typical CMC. There are two types of pores presents in the fiber bundles and matrix of material: (i) The nanopores, the diameter of which is a few nanometers, and they exist in the matrix around the particles; (ii) The micropores, with a few microns in diameter, usually appear in the fiber bundles, matrix and interface.

capturing the effects of microstructural damage is key to describe the deformation and damage behaviors of CMCs. The principal damage mechanisms operative in CMCs and their evolution during thermomechanical loading are illustrated in Fig. 2.

There are three types of microstructural damages in the composites:

(i) The microcracks, which exist in the matrix due to severe local thermal stresses, and they tend to propagate rapidly at the level of the warp and weft threads across the entire width of fiber spacing. The matrix cracking can produce inelastic strain.
(ii) The nucleation of pores, presents both in the matrix and fiber bundles. The SEM observation has confirmed that there is hierarchical porosity in the matrix and fiber bundles, and the nucleation of pores will lead to the decrease of material property during the thermomechanical loading.
(iii) The fiber breaking, exist in the fiber bundles. As the fiber bundles consist of fibers and matrix that encloses fibers, when the fiber breaking occurs, the load on the fiber will transfer to other fibers, which will lead to the degeneration of the carrying capacity for fiber bundles.

Generally, under thermomechanical loading, the microstructural damage evolution for CMCs can be categorized into three stages: Originally, the material is at the initial stage without any loading, and there are some original cracks and micropores can be observed which are formed in the manufacturing process. Then, during the thermomechanical loading, the thermal stress will generate in the material, and the different temperatures in the internal and external of material induce the stress, which therefore results in the generation and expansion of the original cracks and micropores. Besides, the thermal stress also causes the fiber breaking in the fiber bundles, all of the microstructural changes will lead to the rapid degeneration of the elastic property. Finally, the material reaches the saturation stage. Whatever the thermomechanical loading increases, both the crack density and microporosity increases to the saturation level, and the property of material practically impossible to decrease.

There are great challenges in describing the damage failure mechanism and its driving mode of CMCs under thermomechanical loading, due to that: (i) the thermal structural uncertainty of CMCs has multi-level and multi-source characteristics; (ii) the complex structure leads to different and possibly coupled damage mechanisms in the materials; (iii) the models describing these damage mechanisms are presented cross-scale features from compositional length (m scale) to part feature length (cm scale). Therefore, the micromechanics-based models have been developed, which relate the component properties to the overall response of composites. These models represent the damage in a physically realistic way by explicitly modeling matrix cracks or fiber breaks. However, the micromechanics-based models are difficult to scale to coarser scales. The main problem is that damage cannot be clearly represented on a coarse scale (such as matrix crack formation in transverse layers, crack propagation to axial layers, debonding/slipping, fiber fragmentation). In view of this, in the current work, the experimental test data is combined with the theoretical model to try to reveal the physical mechanism behind the damage evolution of the material

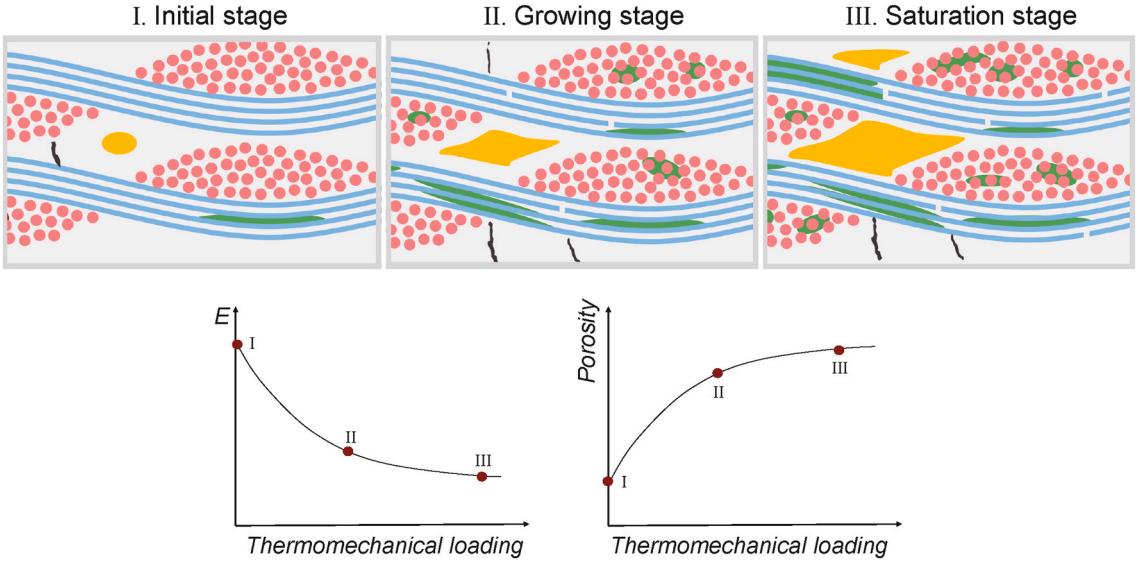

Fig. 2. The principal damage mechanisms operative in CMCs and their evolution during thermomechanical loading.

microstructure through the method of stepwise homogenization.

3. Hierarchical porosity-based elasto-plastic constitutive model

In fact, the hierarchical porosity and micro-cracks in the material can cause the nonlinear stress-strain constitutive behavior. The effective properties of CMCs with hierarchical porosity will be determined, and a elasto-plastic constitutive model will be described in this section. Regarding the hierarchical porosity as the third phase in the material except for the fiber bundles and matrix, the effective elastic property will be described by the homogenization method, and the Gurson-Tvergaard-Needleman (GTN) model is applied to determine the plastic property. It should be mentioned that even though the GTN model is first proposed to describe the plastic behaviors for ductile metal with pores, it has been expand and widely used in composites now [14].

The strain rate in CMCs can be divided into plastic strain rate and elastic strain rate, as:

$$\dot{\boldsymbol{\epsilon}} = \dot{\boldsymbol{\epsilon}}^{e} + \dot{\boldsymbol{\epsilon}}^{p} \tag{3}$$

where $\dot{\boldsymbol{\epsilon}}$ is the total strain rate, $\dot{\boldsymbol{\epsilon}}^{e}$ is the elastic strain rate, $\dot{\boldsymbol{\epsilon}}^{p}$ is the plastic strain rate.

3.1. The elastic behavior of materials

As for the linear isotropic elastic part,

$$\boldsymbol{\sigma} = \mathbf{E}^{e} : \epsilon^{e} \tag{4}$$

where $\boldsymbol{\sigma}$ devotes the Cauchy stress, $\mathbf{E}^{e}$ represents the effective elastic properties. By applied the Mori-Tanaka solution, the effective elastic properties of the composites with hierarchical pores can be obtained.

Assume a representative volume element (RVE) of CMCs with volume V. Then the average stress and strain of the RVE is expressed by,

$$\begin{aligned} \overline{\boldsymbol{\sigma}} &= \zeta_{\mathrm{m}}\overline{\boldsymbol{\sigma}}_{\mathrm{p}}^{\mathrm{m}} + f_{\mathrm{m}}\overline{\boldsymbol{\sigma}}^{\mathrm{m}} + \zeta_{\mathrm{f}}\overline{\boldsymbol{\sigma}}_{\mathrm{p}}^{\mathrm{f}} + f_{\mathrm{f}}\overline{\boldsymbol{\sigma}}^{\mathrm{f}} \\ \overline{\boldsymbol{\epsilon}}^{e} &= \zeta_{\mathrm{m}}\overline{\boldsymbol{\epsilon}}_{\mathrm{p}}^{\mathrm{m}} + f_{\mathrm{m}}\overline{\boldsymbol{\epsilon}}^{\mathrm{m}} + \zeta_{\mathrm{f}}\overline{\boldsymbol{\epsilon}}_{\mathrm{p}}^{\mathrm{f}} + f_{\mathrm{f}}\overline{\boldsymbol{\epsilon}}^{\mathrm{f}} \end{aligned} \tag{5}$$

where $\overline{\boldsymbol{\sigma}}^{\mathrm{f}}, \overline{\boldsymbol{\sigma}}^{\mathrm{m}}$ are the average stress in the fiber bundles and matrix; $\overline{\boldsymbol{\epsilon}}^{\mathrm{f}}, \overline{\boldsymbol{\epsilon}}^{\mathrm{m}}$ are the average strain in the fiber bundles and matrix; $\overline{\boldsymbol{\sigma}}_{\mathrm{p}}^{\mathrm{f}}, \overline{\boldsymbol{\sigma}}_{\mathrm{p}}^{\mathrm{m}}$ are the average stress of pores in the fiber bundles and matrix; $\overline{\boldsymbol{\epsilon}}_{\mathrm{p}}^{\mathrm{f}}, \overline{\boldsymbol{\epsilon}}_{\mathrm{p}}^{\mathrm{m}}$ are average strain of the inclusions (pores) of fiber bundles and matrix; f_{f}, f_{m} are the volume fraction of fiber bundles and matrix. It should be noted that in Eq. (5), the Mori-Tanaka method assumes that the pores can be considered as inclusions in the fiber bundles and matrix, so that they have stress and strain which is actually zero.

Obtained the inclusion theory, the strain of the pores includes the disturbance part $\boldsymbol{\epsilon}_{\mathrm{d}}$, the far-field uniform part $\boldsymbol{\epsilon}_0$ and eigenstrain $\boldsymbol{\epsilon}^{*}$, as the pores considered as inclusions will disturb the homogeneous far-field strain field. Then the strain can be expressed as:

$$\begin{aligned} \boldsymbol{\epsilon}_{\mathrm{p}}^{\mathrm{m}} &= \boldsymbol{\epsilon}_0 + \boldsymbol{\epsilon}_{\mathrm{dp}}^{\mathrm{m}} - \boldsymbol{\epsilon}^{*} \quad \text{in } V_{\mathrm{p}}^{\mathrm{m}} \\ \boldsymbol{\epsilon}_{\mathrm{p}}^{\mathrm{f}} &= \boldsymbol{\epsilon}_0 + \boldsymbol{\epsilon}_{\mathrm{dp}}^{\mathrm{f}} - \boldsymbol{\epsilon}^{*} \quad \text{in } V_{\mathrm{p}}^{\mathrm{f}} \\ \boldsymbol{\epsilon}^{\mathrm{m}} &= \boldsymbol{\epsilon}_0 + \boldsymbol{\epsilon}_{\mathrm{d}}^{\mathrm{m}} - \boldsymbol{\epsilon}^{*} \quad \text{in } V_{\mathrm{m}} \\ \boldsymbol{\epsilon}^{\mathrm{f}} &= \boldsymbol{\epsilon}_0 + \boldsymbol{\epsilon}_{\mathrm{d}}^{\mathrm{f}} - \boldsymbol{\epsilon}^{*} \quad \text{in } V_{\mathrm{f}} \end{aligned} \tag{6}$$

where $V_{\mathrm{p}}^{\mathrm{f}}$ and $V_{\mathrm{p}}^{\mathrm{m}}$ are the volume of pores in the fiber bundles and matrix, V^{f} and V^{m} are the volume of fiber bundles and matrix.

Substituting Eq. (6) into Eq. (4), the stress of pores in the matrix and fiber bundles are,

$$\begin{aligned} \boldsymbol{\sigma}_{\mathrm{p}}^{\mathrm{m}} &= \boldsymbol{E}^{\mathrm{m}} : \left(\boldsymbol{\epsilon}_0 + \boldsymbol{\epsilon}_{\mathrm{dp}}^{\mathrm{m}} - \boldsymbol{\epsilon}^{*}\right) = \boldsymbol{E}_{\mathrm{p}}^{\mathrm{m}} : \left(\boldsymbol{\epsilon}_0 + \boldsymbol{\epsilon}_{\mathrm{dp}}^{\mathrm{m}}\right) \quad \text{in } V_{\mathrm{p}}^{\mathrm{m}} \\ \boldsymbol{\sigma}_{\mathrm{p}}^{\mathrm{f}} &= \boldsymbol{E}^{\mathrm{f}} : \left(\boldsymbol{\epsilon}_0 + \boldsymbol{\epsilon}_{\mathrm{dp}}^{\mathrm{f}} - \boldsymbol{\epsilon}^{*}\right) = \boldsymbol{E}_{\mathrm{p}}^{\mathrm{f}} : \left(\boldsymbol{\epsilon}_0 + \boldsymbol{\epsilon}_{\mathrm{dp}}^{\mathrm{f}}\right) \quad \text{in } V_{\mathrm{p}}^{\mathrm{f}} \end{aligned} \tag{7}$$

where $\boldsymbol{E}^{\mathrm{f}}$, $\boldsymbol{E}^{\mathrm{m}}$ are the stiffness of fiber bundles and matrix, $\boldsymbol{E}_{\mathrm{p}}^{\mathrm{f}}, \boldsymbol{E}_{\mathrm{p}}^{\mathrm{m}}$ are the stiffness of pores in the fiber bundles and matrix. Bedsides, $\boldsymbol{\epsilon}^{*}$ can be used to express the disturbance strain $\boldsymbol{\epsilon}_{\mathrm{d}}^{\mathrm{p}}$:

$$\begin{aligned} \boldsymbol{\epsilon}_{\mathrm{dp}}^{\mathrm{m}} &= \boldsymbol{S}_{\mathrm{m}} : \boldsymbol{\epsilon}_{\mathrm{m}}^{*} \quad \text{in } V_{\mathrm{p}}^{\mathrm{m}} \\ \boldsymbol{\epsilon}_{\mathrm{dp}}^{\mathrm{f}} &= \boldsymbol{S}_{\mathrm{f}} : \boldsymbol{\epsilon}_{\mathrm{f}}^{*} \quad \text{in } V_{\mathrm{p}}^{\mathrm{f}} \end{aligned} \tag{8}$$

where $\boldsymbol{S}_{\mathrm{f}}$, $\boldsymbol{S}_{\mathrm{m}}$ are the function of stiffness and the shape of pores in the fiber bundles and matrix;

Substituting Eq. (8) into Eq. (7), and

$$\begin{aligned} \boldsymbol{\epsilon}_{\mathrm{m}}^{*} &= \left(\boldsymbol{A}_{\mathrm{m}} - \boldsymbol{S}_{\mathrm{m}}\right)^{-1} : \boldsymbol{\epsilon}_0 \\ \boldsymbol{\epsilon}_{\mathrm{f}}^{*} &= \left(\boldsymbol{A}_{\mathrm{f}} - \boldsymbol{S}_{\mathrm{f}}\right)^{-1} : \boldsymbol{\epsilon}_0 \end{aligned} \tag{9}$$

where $\boldsymbol{A}_{\mathrm{m}} = \left(\boldsymbol{E}^{\mathrm{m}} - \boldsymbol{E}_{\mathrm{i}}^{\mathrm{m}}\right)^{-1} : \boldsymbol{E}^{\mathrm{m}}$, $\boldsymbol{A}_{\mathrm{f}} = \left(\boldsymbol{E}^{\mathrm{f}} - \boldsymbol{E}_{\mathrm{i}}^{\mathrm{f}}\right)^{-1} : \boldsymbol{E}^{\mathrm{f}}$. Then the average stress and strain of the pores is rewritten as,

$$\begin{aligned} \overline{\epsilon}_{\mathrm{p}}^{\mathrm{m}} &= \epsilon_0 + \mathbf{S}_{\mathrm{m}} : \left(\mathbf{A}_{\mathrm{m}} - \mathbf{S}_{\mathrm{m}}\right)^{-1} : \epsilon_0 \\ \overline{\epsilon}_{\mathrm{p}}^{\mathrm{f}} &= \epsilon_0 + \mathbf{S}_{\mathrm{f}} : \left(\mathbf{A}_{\mathrm{f}} - \mathbf{S}_{\mathrm{f}}\right)^{-1} : \epsilon_0 \\ \overline{\sigma}_{\mathrm{p}}^{\mathrm{m}} &= \mathbf{E}^{\mathrm{m}} : \left(\epsilon_0 + \left(\mathbf{S}_{\mathrm{m}} - \mathbf{I}\right) : \left(\mathbf{A}_{\mathrm{m}} - \mathbf{S}_{\mathrm{m}}\right)^{-1} : \boldsymbol{\epsilon}_0\right) \\ \overline{\sigma}_{\mathrm{p}}^{\mathrm{f}} &= \mathbf{E}^{\mathrm{f}} : \left(\epsilon_0 + \left(\mathbf{S}_{\mathrm{f}} - \mathbf{I}\right) : \left(\mathbf{A}_{\mathrm{f}} - \mathbf{S}_{\mathrm{f}}\right)^{-1} : \epsilon_0\right) \end{aligned} \tag{10}$$

where $\boldsymbol{I}$ is the fourth order symmetric identity tensor [15]. Substituting Eq. (10) into Eq. (5), and $\boldsymbol{E} = \overline{\boldsymbol{\sigma}} : \overline{\boldsymbol{\epsilon}}^{-1}$, $\boldsymbol{E}_{\mathrm{p}}^{\mathrm{m}} = \boldsymbol{E}_{\mathrm{p}}^{\mathrm{f}} = 0$, the effective stiffness thus is obtained as,

$$\begin{aligned} \mathbf{E} = \left\{f_{\mathrm{m}}\mathbf{E}^{\mathrm{m}} + f_{\mathrm{f}}\mathbf{E}^{\mathrm{f}}\right\} : \\ \left\{\boldsymbol{I} + \zeta_{\mathrm{m}}\mathbf{S}_{\mathrm{m}} : \left(\boldsymbol{I} - \mathbf{S}_{\mathrm{m}}\right)^{-1} + \zeta_{\mathrm{f}}\mathbf{S}_{\mathrm{f}} : \left(\boldsymbol{I} - \mathbf{S}_{\mathrm{f}}\right)^{-1}\right\}^{-1} \end{aligned} \tag{11}$$

Eq. (11) gives the analytical solution of effective elastic property for CMCs with hierarchical pores. However, the complex form limits the application of Eq. (11). Therefore, a scalar form is proposed in the previous work [13],

$$\begin{aligned} E_1 &= \eta_0 E_{\mathrm{f}} \varpi f_{\mathrm{f}} (1 - \zeta_{\mathrm{f}} - \zeta_{\mathrm{m}})^{\mathrm{a}} + E_{\mathrm{m}} f_{\mathrm{m}} (1 - \varpi)(1 - \zeta_{\mathrm{f}} - \zeta_{\mathrm{m}})^{\mathrm{a}} \\ E_2 &= \frac{\eta_0 \left(1 - \zeta_{\mathrm{f}} - \zeta_{\mathrm{m}}\right)^{\mathrm{a}-2} E_{\mathrm{f}} E_{\mathrm{m}}}{\left[\eta_0 (1 - \varpi) E_{\mathrm{f}} f_{\mathrm{m}} + \varpi E_{\mathrm{m}} f_{\mathrm{f}}\right]} \end{aligned} \tag{12}$$

where E_1 and E_2 are the elastic modulus in the principal directions, a is a material parameter obtained by experiments, η_0 represents the influence of the fiber orientation [16]; ϖ devotes a weight factor determined by the porosity in fiber bundles and matrix.

3.2. The plastic behavior of materials

The effective plastic behavior of CMCs is related to the microstructure evolution. It is of importance to understand the plastic behavior when describing the damage initiation and accumulation of materials [17]. To investigate the effective plastic behavior, the hardening law and plastic flow rule will be introduced in this section taken into account the effect of pores in the material. It should be noted that the following description for the hardening law and plastic flow rule is based on the inelastic straining of materials due to the micro-cracking and micropores.

The plastic strain rate is assumed to be normal to the flow potential, as:

$$\dot{\boldsymbol{\epsilon}}_{ij}^{p} = \dot{\gamma} \frac{\partial \Phi}{\partial \boldsymbol{\sigma}_{ij}} \tag{13}$$

where $\dot{\gamma}$ represents the plastic multiplier, Φ devotes the yield function. Considering the presence of pores in the material, the GTN model is applied to determine the macroscopic yield criterion, which is denoted in term of the macroscopic stress,

$$\Phi = \frac{\sigma_{eq}^2}{\sigma_0^2} + 2q_1\zeta\cosh\left(\frac{3q_2\sigma_m}{2\sigma_0}\right) - 1 - q_3(\zeta)^2 \tag{14}$$

where q_1, q_2, q_3 are the model parameters, σ_{eq} is the equivalent stress, σ_m denote the hydrostatic stress, and,

$$\begin{aligned} \sigma_m &= \sigma_{ii}/3 \\ \sigma_{dev} &= \sigma - \sigma_m\delta_{ij} \\ \sigma_{eq} &= \left(\frac{3}{2}\sigma_{dev} : \sigma_{dev}\right)^{1/2} \end{aligned} \tag{15}$$

Applied the chain rule for Eq. (13), then,

$$\frac{\partial\Phi}{\partial\sigma} = \frac{1}{3}\frac{\partial\Phi}{\partial\sigma_m}\mathbf{I} + \frac{\partial\Phi}{\partial\sigma_{eq}}\mathbf{n} \tag{16}$$

where

$$\mathbf{n} = \frac{3}{2\sigma_{eq}}\sigma_{dev} \tag{17}$$

Substituting Eq. (17) into Eq. (16), the flow rule can be rewritten as:

$$\dot{\epsilon}^p = \dot{\gamma}\left(\frac{1}{3}\dot{\epsilon}_m^p I + \dot{\epsilon}_{eq}^p\mathbf{n}\right) \tag{18}$$

The volumetric strain rate caused by the hydrostatic pressure is defined as,

$$\dot{\epsilon}_m^p = \gamma\left(\frac{\partial\Phi}{\partial\sigma_m}\right) = \gamma 3q_1q_2f^*(\zeta)\sinh\left(\frac{3q_2\sigma_m}{2\bar{\sigma}}\right)\frac{1}{\bar{\sigma}} \tag{19}$$

The equivalent plastic strain rate caused by the equivalent pressure is expressed as,

$$\dot{\epsilon}_{eq}^p = \gamma\left(\frac{\partial\Phi}{\partial\sigma_{eq}}\right) = \gamma\frac{2\sigma_{eq}}{\sigma^2} \tag{20}$$

and based on the energy balance, the effective plastic strain rate can be obtained by the porosity,

$$\sigma_y\dot{\bar{\epsilon}}^p(1-\zeta) = \sigma_{ij}\dot{\epsilon}_{ij}^p \tag{21}$$

where σ_y is the average yield stress of the materials.

4. Description of the damage model

The aim of this section is to derive a micromechanical damage model that is able to determine the microstructure damage and its possible evolution of CMCs during thermomechanical loading. From a micromechanical point of view, the macroscopic mechanical behaviors of CMCs are influenced by the combination of three main micromechanical damage mechanisms, namely, the matrix cracking, nucleation of microstructural pores and fiber breaking, as mentioned in Fig. 2. It is significant to figure out the influence of different damage mechanisms on the macroscopic damage behavior.

Thus, the proposed micromechanical damage model should have the ability to (i) capture the basic features of micromechanical damage, such as the nucleation of pores, matrix cracking and fiber breaking, and (ii) supply evolution laws for the damage parameters defining different damage mechanisms. In this case, three micromechanical damage variables, ω_c, ω_p and ω_b, are chosen to represent the micromechanical damage in the materials. ω_c represents the damage due to the activation and propagation of matrix cracking, ω_p relies on the nucleation of pores on account of the increasing strain, and ω_b depends on the breaking of fibers in the fiber bundles under thermomechanical loading. The mechanism and evolution of each damage variable will be briefly discussed in this section, which will be applied to establish the micromechanical damage evolution models in the fiber bundles and matrix.

4.1. Matrix cracking

In the process of thermomechanical loading, the microcracks will active and propagate the matrix, due to the severe thermal stress caused by rapid temperature change. Besides, matrix cracks induced by the thermomechanical loading can be related to the inelastic deformation of materials [2,18]. During the thermomechanical loading, the cracks in the matrix generate and tend to propagate across the width of the matrix layer between fiber layers. The width is defined as the length of each crack, as described in Fig. 3. The damage due to the matrix cracking is related to the multiplication of matrix cracks.

Assuming that the cracks in the matrix are homogeneously distributed, and the crack density is continuous as the increment of crack density is small, then the proposed damage variable ω_c can be defined as the crack density, and the determination of ω_c is related to the geometry of a cracks system and the distance between two cracks. Consider a cracks system as shown in Fig. 3, the number of cracks is n, and the deep of each crack is $2a$, the thick is $2b$, then,

$$n = L\frac{\omega_c}{2a} \tag{22}$$

where L is the length of the cracks system. It is recognized that the plastic strain can be related to the crack opening displacements in the cracks system, which can be expressed by the following relationship [18]:

$$\epsilon^{\mathrm{p}} = \frac{\Delta L^{\mathrm{in}}}{L} = \frac{n\cdot 2U}{L} = \frac{n\cdot 2b}{L} = \delta\cdot\omega_c \tag{23}$$

where U is the total crack opening displacements, and δ is the aspect ratio of a crack, $\delta = b/a$. Therefore, the plastic strain can be obtained by multiplying the crack density and the aspect ratio of a crack. From Eq. (22), the damage variable of matrix cracking can be defined as:

$$\omega_c = \frac{\epsilon^{\mathrm{p}}}{\delta} \tag{24}$$

By differentiating Eq. (24) with time, the matrix cracking damage temporal evolution can be determined,

$$\dot{\omega}_c = \frac{\dot{\epsilon}^{\mathrm{p}}}{\delta} \tag{25}$$

Therefore, the damage evolution of the matrix cracking can be obtained by Eq. (25) as long as the plastic strain is determined.

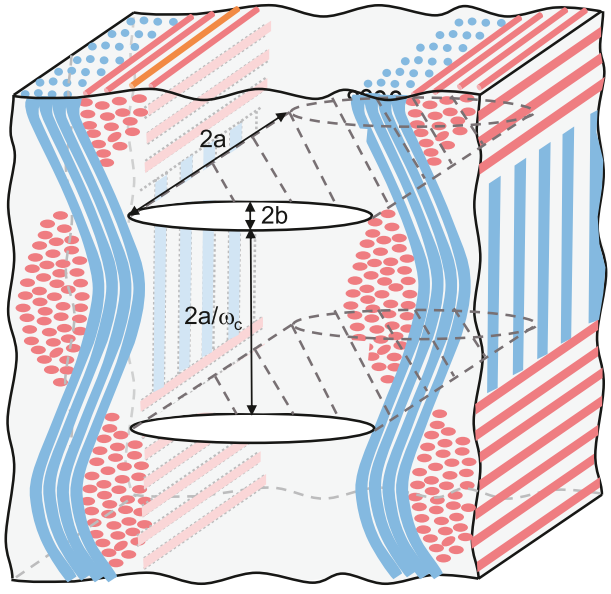

Fig. 3. The cracks in the matrix of CMCs.

4.2. Nucleation of micropores

As mentioned above, there are two populations of pores in the materials, and the nucleation and growth of the hierarchical pores during the thermomechanical loading will lead to the decrease of carrying capacity, as well as the material property. To investigate the damage caused by nucleation and growth of the hierarchical pores, as in Ref. [13], simplifying assumptions for the hierarchical porosity are listed in the following:

(i) The volume fraction of nanopores is assumed to be constant when suffering from the thermomechanical loading, as the nucleation and growth of nanopores can be neglected.
(ii) The micropores distribute in the fiber bundles and matrix, therefore the nucleation of micropores needs to be considered in the different components.

The rate of the microporosity evolution includes the rate of change of pore volume fraction caused by original void growth $\dot{\zeta}_g$ and new void nucleation $\dot{\zeta}_n$:

$$\dot{\zeta} = \dot{\zeta}_g + \dot{\zeta}_n \tag{26}$$

As the matrix is brittle, the growth of voids can be ignored, so that $\dot{\zeta} = \dot{\zeta}_n$, and the change rate of microporosity caused by nucleation adopts the shape approval rule of strain control,

$$\dot{\zeta}_n = A\dot{\bar{\epsilon}}^{pl} \tag{27}$$

where $\bar{\epsilon}^{pl}$ is the microscopic equivalent plastic strain, and

$$A = \frac{f_N}{s^N\sqrt{2\pi}}\exp\left[-\frac{1}{2}\left(\frac{\bar{\epsilon}^{pl}-\epsilon_N}{s_N}\right)^2\right] \tag{28}$$

where f_N is the volume fraction of a nucleated void, ϵ_N is the average equivalent plastic strain of a nucleated void, and s_N is the standard deviation of a nucleated void.

Referring to Ref. [19], the material entropy dissipation rate can be used to describe the evolution of porosity, then the temporal evolution of ω_p is expressed as,

$$\dot{\omega}_p = \frac{1}{\epsilon_v}\frac{|\dot{\zeta}_n|}{(1-\zeta)}H(1-\omega_p) \tag{29}$$

$H(x)$ is the Heaviside function, and,

$$H(x) = \begin{cases} 0 & \text{for } x \leqslant 0 \\ 1 & \text{for } x > 0 \end{cases}$$

the Heaviside function ensures that ω_p always less than 1.

4.3. Breaking of fibers

Fiber bundles in CMCs include a large amount of fibers. During the thermomechanical loading, the breaking of fibers will occur, generating decohesions and slips at the fiber-matrix interfaces, and leads to the decrease of carrying capacity of fiber bundles even the failure of fiber bundles. Therefore, the damage caused by fiber breaking should take into consideration.

Considering a fiber bundle subjected to global loading, when the fiber breaking occurs, the failed fiber will not bear the load, and it will transmit to the intact fibers. The fracture probability of fibers can be used to express the fiber breaking damage, drawing on W. Weibull's idea [20],

$$\mathcal{F}\left(\sigma_f^*\right) = 1 - \exp\left\{-V\left(\frac{\sigma_f^*}{\sigma_w}\right)^{\alpha}\right\} \tag{30}$$

where σ_f^* is the stress of fibers, σ_w is the scale parameter, and α is the shape parameter; V means the volume of fibers. Assuming that the number of fibers in a fiber bundle is ϱ, and the number of break fibers can be expressed by the fracture probability of fibers,

$$\varrho_b = \mathcal{F}\left(\sigma_f^*\right)\varrho \tag{31}$$

therefore, the number of intact fibers is $\varrho - \varrho_b = \left(1 - \mathcal{F}\left(\sigma_f^*\right)\right)\varrho$.

For fibers, the probability density of fibers is assumed to be the fiber breaking damage variable, ω_f, then $\omega_f = \mathcal{F}\left(\sigma_f^*\right)$. Therefore, the fiber breaking damage evolution can be obtained by Eq. (30),

$$D_f = 1 - \exp\left\{-\left(\frac{E_f^0\epsilon_f}{\sigma_w}\right)^{\alpha}\right\} \tag{32}$$

4.4. Damage evolution of fibers and matrix

As mentioned above, the damage mechanisms in the fiber bundles and matrix are not the same, it is of importance to consider the thermomechanical damage evolutions in the fiber bundles and matrix respectively. Two damage variables are introduced to the damage of fiber bundles and matrix.

$$\begin{aligned} D_m &= 1 - (1-\omega_c)\left(1-\omega_p^m\right) \\ D_f &= 1 - \left(1-\omega_f\right)\left(1-\omega_p^f\right) \end{aligned} \tag{33}$$

where D_m is the damage of matrix, D_f is the damage of fiber bundles, and ω_p^m devotes the nucleation of matrix microporosity, ω_p^f represents the nucleation of fibers microporosity. Eq. (33) illustrates that there are two damage mechanisms in the matrix: matrix cracking and nucleation of matrix microporosity; Similarly, the damage mechanisms considered in the fiber bundles are fiber breaking and nucleation of fibers microporosity.

The damage evolution of fiber bundles and matrix is conducted under the thermodynamic framework. The Helmholtz free energy of CMCs is expressed as a function of state variables, including the internal state variables (α) and external state variables (ϵ^e and T):

$$\psi = \widehat{\psi}(\epsilon^e, T, \alpha) \tag{34}$$

Consider the elasto-plastic behaviors of CMCs, the Helmholtz free energy can be separated into plastic and elastic parts, as,

$$\psi = \psi_e(\epsilon^e, D) + \psi_p\left(\alpha_j, D\right) \tag{35}$$

where D is the total damage of CMCs. By extracting the total damage, the Helmholtz free energy can be rewritten as,

$$\psi = (1-D)\left[\psi_e(\epsilon^e) + \psi_p\left(\alpha_j\right)\right] \tag{36}$$

and

$$\psi_e = \frac{1}{\rho}\left(\frac{1}{2}\epsilon_{ij}\sigma_{ij} + \alpha(T-T_0)\right) \tag{37}$$

where α is the thermal expansion coefficient. The corresponding effective stresses are,

$$\sigma_{ij} = \rho\frac{\partial\psi}{\partial\epsilon_{ij}} = C_{ijkl}\epsilon_{kl}^e(1-D)) \tag{38}$$

where C_{ijkl} is the fourth-order stiffness tensor, and has been discussed in the previous section.

The strain energy density release rate Y can be used to determine the damage evolution in the fiber bundles and matrix, containing two additive terms, and is defined as,

$$Y = -\rho\frac{\partial\psi}{\partial D} = Y_e + Y_p = -\rho\frac{\partial\psi_e}{\partial D} - \rho\frac{\partial\psi_p}{\partial D} \tag{39}$$

The strain energy density release rate of matrix and fiber bundles can be expressed as:

$$Y_m = -\rho\frac{\partial\psi_m}{\partial D_m}, Y_f = -\rho\frac{\partial\psi_f}{\partial D_f} \tag{40}$$

where Y_m and Y_f are the strain energy density release rate of matrix and fiber bundles, respectively, and ψ_m and ψ_f are the Helmholtz free energy of matrix and fiber bundles, respectively.

As the damage evolution of fiber bundles and matrix can be described under the same framework, the damages of matrix and fiber bundles are expressed as D_i in the following description for the sake of argument, and the subscript i can be replaced by m or f for matrix or fiber bundles. To determine the relationship between the strain energy density release rate and damage, and the damage evolution, the power law has been used in the damage models, which can not describe damage evolution accurately. Therefore, the potential function is used to describe the damage evolution under thermomechanical loading,

$$\mathscr{F}(D_i) = Y_i - \mathscr{L}(D_i), \tag{41}$$

where $\mathscr{L}(D_i)$ devotes the material resistance against damage, when the strain energy density release rate Y_i equals to the material resistance $\mathscr{L}(D_i)$, the damage occurs. The material resistance $\mathscr{L}$ is described as [13],

$$\mathscr{L} = Y_{th,\ i} + \exp\left(\frac{D_i}{\beta_i D_i^{cr}}\right) \tag{42}$$

where D_i^{cr} devotes the maximum damage value leading material failure, β_i is a model parameter, $Y_{th,i}$ is the threshold of Y_i.

Referring to the maximum dissipation principle, the damage evolution law can be expressed as,

$$\dot{D}_i = \dot{\lambda}_i\frac{\partial\mathscr{F}(D_i)}{\partial Y_i} = \dot{\lambda}_i. \tag{43}$$

where $\dot{\lambda}_i$ is the damage multiplier, and

$$\begin{cases} \dot{\lambda}_i \ \geq 0 & \text{for} \quad \mathscr{F}(Y_i, D_i) = 0, \\ \dot{\lambda}_i \ = 0 & \text{for} \quad \mathscr{F}(Y_i, D_i) < 0, \end{cases} \tag{44}$$

The damage multiplier is non-negative for thermomechanical loading, and can be obtained by the damage consistency condition,

$$\mathrm{d}\mathscr{F}(D_i) = \frac{\partial\mathscr{F}(D_i)}{\partial Y_i}\dot{Y}_i - \frac{\partial\mathscr{L}}{\partial D_i}\dot{\lambda}_i = 0. \tag{45}$$

Therefore, the damage evolution law is obtained,

$$\dot{D}_i = \frac{D_i^{cr}\beta_i}{Y_i}\dot{Y}_i, \tag{46}$$

Integrating Eq. (46) over $[Y_{th,i}, Y_i]$, the explicit damage expression can be obtained,

$$D_i = D_i^{ini} + D_i^{cr}\left[\beta_i \ln Y_i - \beta_i \ln Y_{th,i}\right] \tag{47}$$

Eq. (47) shows the damage evolution law of fiber bundles and matrix in CMCs. If the parameter β_i, $Y_{th,i}$, D_i^{ini}, D_i^{cr} are determined, then the damage evolution can be obtained easily.

The damage model in Eq. (47) contains four material parameters to be identified, which have physical meaning: the model parameter β, the critical damage D_i^{cr}, the initial damage D_i^{ini} and the threshold strain energy release rate $Y_{th,i}$. The determination of the four parameters can be obtained by conducting simple uniaxial test.

In fact, the damage as a function of the strain energy density release rate can be obtained using a logarithmic plot $\left(D_i - D_i^{ini}\right)D_i^{cr}$ versus $\left(\ln Y_i - \ln Y_{th,i}\right)$, the meaning of the slope of the best linear fit is the value of the damage exponent β, as

$$\frac{D_i - D_i^{ini}}{D_i^{cr}} = \beta_i\left(\ln Y_i - \ln Y_{th,i}\right) \tag{48}$$

Then β can be obtained from the available experimental data.

Therefore, a theoretical model for the micromechanical damage of CMCs under thermomechanical loading is established, and both the matrix and fiber damage are investigated by the damage evolution model, which is extracted from micro-characterization and monotonic tensile tests. It should be mentioned that, during the experimental process with high temperature (greater than 1000 °C), it is impossible to observe the internal damage-deformation behavior of the material during cyclic thermal shock from both macroscopic and microscopic perspectives, due to the limitation of the temporal and spatial resolution of the existing experimental methods. Therefore, the load form of cyclic thermal shock is used in the current study, which means that the material is subjected to cyclic thermal shock test firstly, and then characterized at room temperature. The details of the specific experiment and characterization can refer to some of earlier works [3,17]. Meanwhile, the acoustic emission method can detect the onset and qualitative of damage, but the attribution of acoustic events to different physical phenomena requires in-depth interpretation. Given the above challenges, the mercury intrusion method to test the evolution of the internal pores of the material to characterize the matrix cracks. As for fiber fracture, the proposed damage model is based on the fiber probabilistic fracture damage model developed by Curtin [23] and Jacques Lamon [24], and is modified by considering the influence of local stress state on fiber breakage.

5. Assessment of the damage model through an illustrative application

To verify the applicability of the proposed damage model to CMCs in practical thermomechanical damage problems, and to provide an assessment towards experimental results, the predicted results of the proposed damage model are compared with experimental results received by the oxide/oxide CMCs. This material contains uncoated α-Al_2O_3 fibers and Al_2O_3–SiO_2–ZrO_2 matrix [25]. The total porosity of CMCs varies from 20% to 40%. Table 1 lists the properties of CMC's components used in the damage model.

The thermomechanical loading is applied to the material by cyclic thermal shock tests. Due to the application of CMCs, the temperature of cyclic thermal shock test is 1100 °C. Besides, the specimens were put into the Micromeritics Autopore IV 9510 porosimeter to measure the hierarchical porosity after each thermal shock, and the variation of the pore size distribution of CMCs was generated. The mechanical properties of thermal shocked CMCs can be quantified by the uniaxial monotone tensile test.

5.1. Microstructure observation

The microstructure of composite materials exhibits great heterogeneities with the fibrous texture, the matrix and porosity. Understanding the damage to these porous materials requires a three-dimensional

Table 1
The properties of CMC's components used in the damage model ([21,22]).

Parameter	Symbol	Value	Unit
Elastic modulus of fiber bundles	E_f	379	GPa
Elastic modulus of matrix (porosity-free)	E_m	210	GPa
Density of fiber bundles	ρ_f	4.2	g/cm^3
Density of matrix	ρ_m	4.0	g/cm^3
Volume fraction of fiber bundles	V_f	44	%
Porosity of the composite	ζ	27.6	%
Thermal expansion coefficient of fiber bundles	α_f	8.8×10^{-6}	/°C
Thermal expansion coefficient of matrix	α_m	10.2×10^{-6}	/°C

visualization of materials. Micro/nano-CT technique provides access to three-dimensional information about the object of study. The 3D visualization of the damage (Fig. 4) offers a better understanding for the role of the microstructure change on the mechanical behaviors using the medium-resolution (3.8 μm voxel) laboratory tomography data. The damage mechanisms occurring inside composite materials are visualized such as matrix cracking, micropores, delaminations or even fiber breaks.

Fig. 4(a) illustrates the tomographic visualization of an ox/ox-CMCs specimen subjected to thermomechanical loading, and there are some hierarchical pores that can be observed as well as matrix cracks. To obtain the hierarchical porosity in the material, segmentation of the porosity via image intensity thresholding was achieved by the Avizo Fire software, and the pore distribution in the material is demonstrated in Fig. 4(b). It is observed that the major part of porosity is included in the matrix, and most of them are microporosity. Besides, there are some microporosity existing in the fiber bundles, due to the lack of matrix. The distributions of pores along the different directions are shown in Fig. 4 (c).

5.2. Characterization of the matrix damage

5.2.1. Microstructural damage in the matrix

As discussed in section 3, there are two damage types in the matrix: matrix cracking and nucleation of micropores. The damage caused by matrix cracking is obtained by calculating the inelastic strain of the matrix, and the damage of the nucleation of micropores is obtained by measuring the microporosity in the matrix during thermal shocks. Fig. 5 illustrates the microstructural damage evolution in the matrix of CMCs during cyclic thermal shocks.

Data relating to damage due to matrix microcracking obtained from the damage model are shown in Fig. 5(a). As the original matrix has many pores formed in the manufacturing process, the original porosity is high, with no damage from nucleation of pores. During the thermomechanical loading, microporosity increases with the thermal shocks, and damage from the nucleation of pores increases rapidly. The maximum value of ω_p^{m} is about 0.08. Besides, there is a linear relationship between the porosity in the matrix and the damage from nucleation of pores. Fig. 5(b) illustrates the damage from microcracking obtained from the damage model. The microcracking damage ω_c follows a similar trend. In the process of thermomechanical loading, rapid temperature changes lead to thermal stresses in the matrix, and microcracks tends to generate and propagate rapidly inside the matrix, causing the degeneration of the matrix property. The maximum value of microcracking damage ω_c is about 0.17, which means that the damage due to matrix microcracking plays a leading role in the damage of matrix during thermomechanical loading.

5.2.2. Damage evolution of matrix

The damage evolution model of the matrix is obtained through the above derivation, which can be written as,

$$D_{\mathrm{m}} = D_{\mathrm{m}}^{\mathrm{ini}} + D_{\mathrm{m}}^{\mathrm{cr}}\left[\beta_m \ln Y_{\mathrm{m}} - \beta_m \ln Y_{\mathrm{th,m}}\right] \tag{49}$$

which considers the influences of matrix pore nucleation and matrix cracking. After obtaining the microstructural damage in the matrix, the total damage in the matrix D_{m} can be determined using Eq. (33).

Firstly, the parameters in the evolution model should be determined, and the acquisition of the parameters has been described above. Fig. 6 shows the identification of the model parameter β_{m}, and the slope of the best linear fit is the value of the model parameter β_{m}, as $\beta_{\mathrm{m}} = 0.99$.

Fig. 7 demonstrates the evolution of matrix damage with the strain

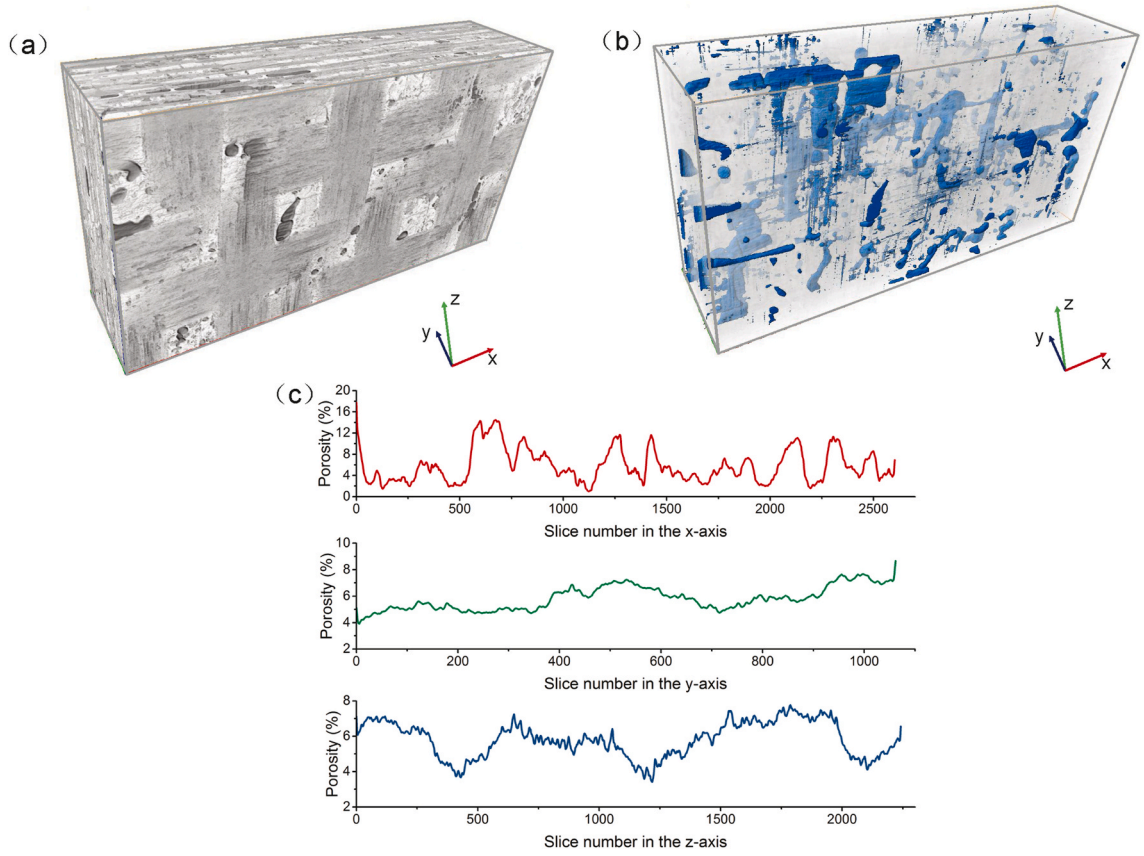

Fig. 4. Tomographic visualization of a CMCs composite subjected to thermomechanical loading; a) Volume reconstruction of the microstructure in the initial state, b) Representation of the hierarchical pores present in the material, c) The porosity versus slice number in different directions. (a) Damage from nucleation of matrix pores vs. porosity. (b) Damage from matrix microcracking vs. inelastic strain

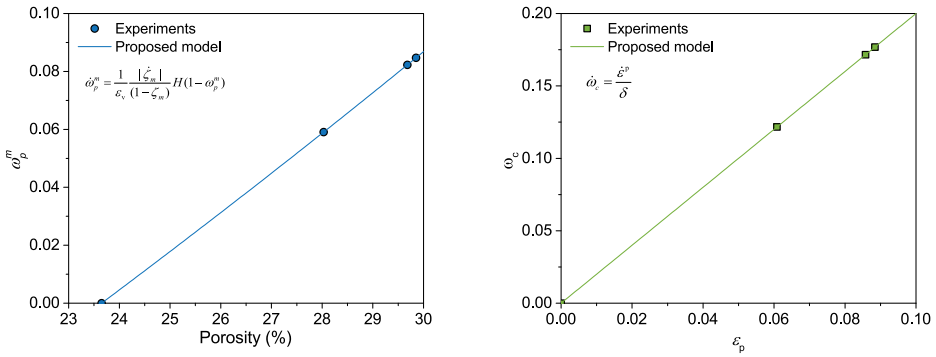

(a) Damage from nucleation of matrix pores vs. porosity (b) Damage from matrix microcracking vs. inelastic strain

Fig. 5. Microstructural damage in the matrix of CMCs.

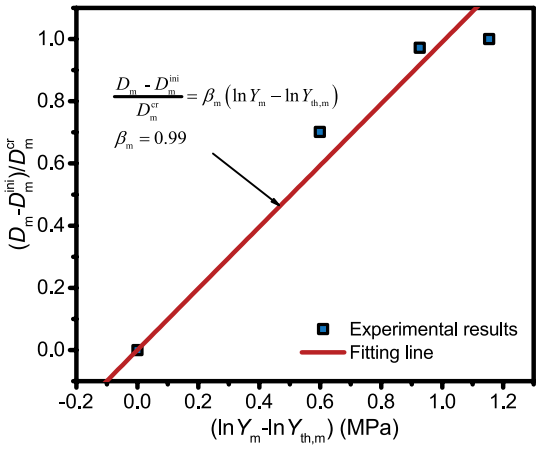

Fig. 6. The identification of the model parameter β_m, where the slope of the fitting line is the value of β_m.

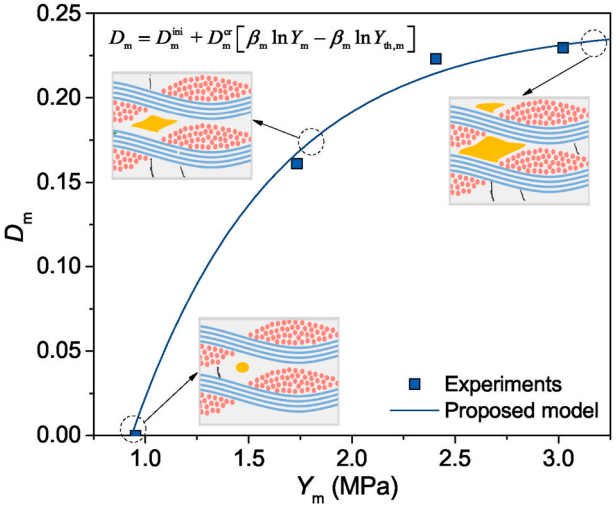

Fig. 7. Evolution of matrix damage with the strain energy release rate Y_m for the CMCs under cyclic thermal shocks, and the predicted results by the proposed model are compared with the experimental results. (a) Damage from nucleation of pores vs. porosity. (b) Damage from fiber breaks vs. strain

energy release rate Y_m for the CMCs under cyclic thermal shocks, and the predicted results by the proposed model are compared with the experimental results. The relationship between the strain energy release rate and the damage is nonlinear, which is due to the microstructure response. It can be seen that the thermomechanical damage in the matrix generates at the threshold strain energy release rate $Y_{\mathrm{th,m}} = 0.8$, at which the micropores in the matrix start to nuclear, in correspondence with the generation of matrix cracking. As Y_m increases, the microporosity in the matrix increases rapidly with newly formed pores, as well as the matrix crack density, leading to the matrix damage accumulates rapidly. Furthermore, when Y_m reaches 3.1 MPa, the microporosity and crack density no longer increase, and the damage reaches a saturation stage, $D_\mathrm{m}^{\mathrm{cr}} = 0.22$. Further loading will leads to the final failure of the matrix. Besides, it is obvious that the predict results of the damage model of matrix agree with the experimental results.

5.3. Characterization of the fiber bundles damage

5.3.1. Microstructural damage in the fiber bundles

The damage in the fiber bundles includes two forms: nucleation of micropores in the fiber bundles and fiber breaking. The damage caused by fiber breaking is obtained by the strain of the fibers, and the damage of the nucleation of micropores is obtained by measuring the microporosity in the fiber bundles during thermal shocks. Fig. 8 shows the microstructural damage evolution of the fiber bundles in CMCs during cyclic thermal shocks.

As shown in Fig. 8(a), damage due to the nucleation of micropores in the fiber bundles increases linearly with microporosity, and the original fiber bundles have fewer pores than the matrix. The maximum value of ω_p^{f} is about 0.05. Similarly, the data of damage due to fiber breaking is demonstrated in Fig. 8(b). The nonlinear relationship between ω_b and strain can be observed, and there are three stages for the damage changes: As ϵ_f changes from 0 to 0.32%, there are only a little crack exists in the fiber bundles, and the damage increases slowly. When ϵ_f is 0.32%–1%, fiber breaking starts to increase rapidly, which are multiple cracks exist in the fiber bundles in the beginning, and with the cracks extend across the fiber section, the fiber breaks, resulting in the damage increases rapidly. As the ϵ_f increases continuously, the fiber breaking occurs in the fiber bundles, and the loading will redistributed to the intact fibers in the fiber bundles. When ϵ_f reaches 1%, the fiber breaking reaches a stable stage, which may lead to the failure of fiber bundles, and the damage no longer increase.

5.3.2. Damage evolution of fiber bundles

Similarly, the damage evolution of the fiber bundles can be obtained after determining the damage of micropore nucleation and fiber breaking, as

$$D_\mathrm{f} = D_\mathrm{f}^{\mathrm{ini}} + D_\mathrm{f}^{\mathrm{cr}}\left[\beta_\mathrm{f}\ln Y_\mathrm{f} - \beta_\mathrm{f}\ln Y_{\mathrm{th,f}}\right] \tag{50}$$

there are four parameters that need to be determined, and they can

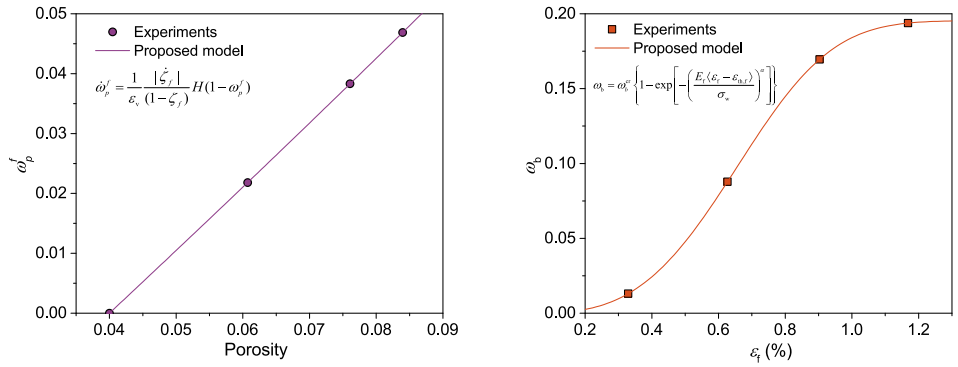

(a) Damage from nucleation of pores vs. porosity (b) Damage from fiber breaks vs. strain

Fig. 8. Microstructural damage in the fiber bundles of CMCs.

describe the effect of the microstructural damage accurately. The acquisition of the model parameters has also been described. The model parameter β_f is identified as illustrated in Fig. 9, where the slope of the linear fit is β_f, and $\beta_f = 0.85$.

Fig. 10 shows the damage evolution of fiber bundles in CMCs with the strain energy release rate Y_f, and the predicted results are compared with experimental results. The damage evolution in the fiber bundles includes three stages: During the initial stage, the damage occurs when Y_f reaches the threshold value $Y_{th,f} = 1.7$, and the damage mechanism mainly is the nucleation of micropores; Then with the Y_f increases, the cracks occur in the fiber bundles, leading to the breaking of fiber, and the micropores in the fiber bundles are nucleated continuously, all of which cause the damage accumulates rapidly. In the final state, as Y_f is 5–5.5 MPa, the damage reaches a saturated state, and the microporosity in the fiber bundles no longer increase, as well as the fiber breaking, the critical damage value is 0.23. In addition, the comparison between the proposed damage model and the experiments indicates the proposed damage model can predict the damage in the fiber bundles.

The discussion of the comparation results shows that the developed damage model has the capability to predict the microstructural damage behaviors of CMCs during thermomechanical loading.

6. Conclusions

In the present work, a new micro-mechanical damage model is established within a thermodynamic framework to describe the microstructural damage behaviors of CMCs under thermomechanical loading. This model couples the damage mechanism in the matrix, which captures the matrix cracking and nucleation of pores, with the damage mechanism in the fiber bundles, which captures the void nucleation and fiber breaking. An illustrative application is performed by experiments to verify the correctness of the proposed damage model. Compared with existing works and the previous works of the author, the key improvement of the present model is that it explicitly takes into account the effects of matrix cracking, hierarchical porosity nucleation, and fiber breaking. The new damage model allows a more realistic description of microstructural damage for a large number of porous composites. The main conclusions are as follows:

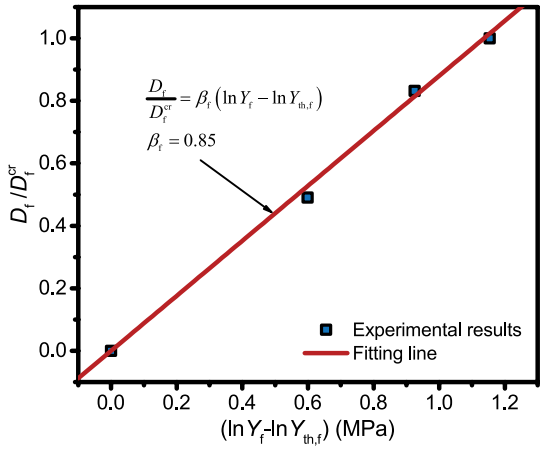

Fig. 9. The identification of β_f for fiber bundles damage evolution, where the slope of the fitting line is the value of β_f.

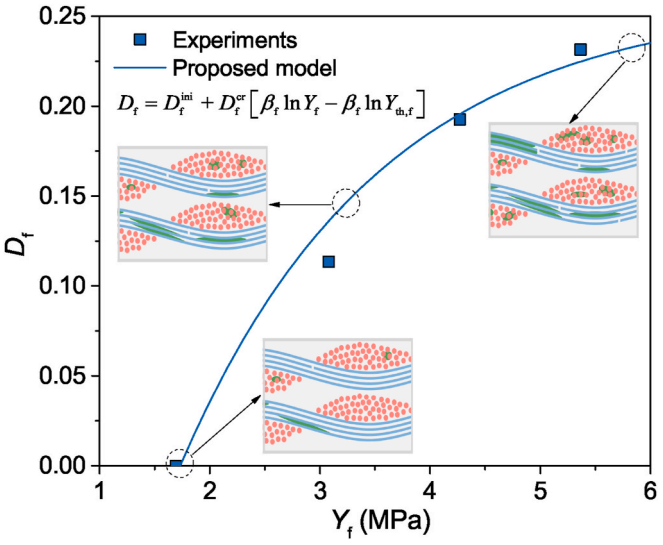

Fig. 10. Damage evolution of fiber bundles in CMCs with the strain energy release rate Y_f, and the predicted results are compared with experimental results.

- The hierarchical porosity leads to the nonlinear constitutive behavior of materials. Therefore, a hierarchical porosity-based elasto-plastic constitutive model was developed based on the homogenization method and the GTN model, and the effects of hierarchical porosity in the fiber bundles and matrix of CMCs has been investigated.
- The principal damage mechanisms for CMCs are the matrix cracking, fiber breaking and microporosity nucleation, and the effects of them were described using three damage variables. The matrix cracking damage variable captures the effect of crack density and is obtained using inelastic strain; The microporosity nucleation damage variable

is a function of the porosity increment; The fiber breaking damage variable depends on the strain in the fiber bundles.

- A micromechanical damage model is established to determine the damage evolution in the fiber bundles and matrix. The porosity nucleation and matrix cracking are considered in the matrix damage, and the fiber breaking and porosity nucleation are included in the fiber bundles damage. Besides, the evolution laws of different damage mechanisms in components are determined and considered in the proposed damage model.
- The verification of the present damage model was conducted by comparing with the experimental results of a typical CMCs. The predict results of the proposed damage model are in good agree with the experimental results, which indicates that the developed damage model has the capability to predict the microstructural damage behaviors of CMCs during thermomechanical loading.

Declaration of competing interest

The authors declare that they have no known competing financial interests or personal relationships that could have appeared to influence the work reported in this paper.

Acknowledgement

The present work is supported by the National Natural Science Foundation of China (NSFC) (Grant No. 52105165), and the Strategic Priority Research Program of Chinese Academy of Sciences (Grant No. XDA17030100).

References

[1] Varun P. Rajan, Frank W. Zok, Matrix cracking of fiber-reinforced ceramic composites in shear, J. Mech. Phys. Solid. 73 (3–21) (2014).
[2] Unni Santhosh, Jalees Ahmad, Greg Ojard, Imelda Smyth, Yasser Gowayed, Jefferson George, Effect of porosity on the nonlinear and time-dependent behavior of ceramic matrix composites, Compos. B Eng. 184 (2020), 107658.
[3] Zhengmao Yang, Hui Liu, A continuum fatigue damage model for the cyclic thermal shocked ceramic-matrix composites, Int. J. Fatig. 134 (2020), 105507.
[4] S. Salekeen, J.N. Amoako, H. Mahfuz, S. Jeelani, Mechanical property degradation of a nicalon fiber reinforced sinc ceramic matrix composite under thermal shock loading, Compos. Struct. 78 (4) (2007) 477–485.
[5] C. Kastritseas, P.A. Smith, J.A. Yeomans, Thermal shock fracture in cross-ply fibre-reinforced ceramic-matrix composites, Phil. Mag. 90 (31–32) (2010) 4209–4226.
[6] W.Q. Shen, J.F. Shao, D. Kondo, B. Gatmiri, A micro-macro model for clayey rocks with a plastic compressible porous matrix, Int. J. Plast. 36 (2012) 64–85.
[7] W.Q. Shen, J.F. Shao, An incremental micro-macro model for porous geomaterials with double porosity and inclusion, Int. J. Plast. 83 (2016) 37–54.
[8] A. Shojaei, G.Q. Li, J. Fish, P.J. Lan, Multi-scale constitutive modeling of ceramic matrix composites by continuum damage mechanics, Int. J. Solid Struct. 51 (23–24) (2014) 4068–4081.
[9] Hoi Kil Choi, Myeong Jin Son, Eui Sup Shin, Jaesang Yu, Prediction of thermo-poro-elastic properties of porous composites using an expanded unmixing-mixing model, Compos. Struct. 188 (2018) 387–393.
[10] Giang D. Nguyen, Ha H. Bui, A thermodynamics-and mechanism-based framework for constitutive models with evolving thickness of localisation band, Int. J. Solid Struct. 187 (2020) 110–120.
[11] Naigeng Chen, Meredith N. Silberstein, A micromechanics-based damage model for non-woven fiber networks, Int. J. Solid Struct. 160 (2019) 18–31.
[12] Travis Skinner, Ashwin Rai, Aditi Chattopadhyay, Multiscale ceramic matrix composite thermomechanical damage model with fracture mechanics and internal state variables, Compos. Struct. 236 (2020), 111847.
[13] Zhengmao Yang, Yan Han, Guian Qian, Zhongdong Ji, Influence of hierarchical porosity on the mechanical properties of porous woven composites under thermomechanical loading, Int. J. Solid Struct. 200–201 (2020) 13–22.
[14] Khaoula Dorhmi, Léo Morin, Katell Derrien, Zehoua Hadjem-Hamouche, Jean-Pierre Chevalier, A homogenization-based damage model for stiffness loss in ductile metal-matrix composites, J. Mech. Phys. Solid. 137 (2020), 103812.
[15] Hansong Huang, Talreja Ramesh, Effects of void geometry on elastic properties of unidirectional fiber reinforced composites, Compos. Sci. Technol. 65 (13) (2005) 1964–1981.
[16] Behnaz Baghaei, Mikael Skrifvars, Masoud Salehi, Tariq Bashir, Marja Rissanen, Pertti Nousiainen, Novel aligned hemp fibre reinforcement for structural biocomposites: porosity, water absorption, mechanical performances and viscoelastic behaviour, Compos. Appl. Sci. Manuf. 61 (2014) 1–12.
[17] Zhengmao Yang, Hui Liu, An elastic-plastic constitutive model for thermal shocked oxide/oxide ceramic-matrix composites, Int. J. Mech. Sci. 175 (2020), 105528.
[18] Stéphane Baste, Inelastic behaviour of ceramic-matrix composites, Compos. Sci. Technol. 61 (15) (2001) 2285–2297.
[19] M.B. Rubin, O.Y. Vorobiev, L.A. Glenn, Mechanical and numerical modeling of a porous elastic-viscoplastic material with tensile failure, Int. J. Solid Struct. 37 (13) (2000) 1841–1871.
[20] E. Benjamin Callaway, Frank W. Zok, Tensile response of unidirectional ceramic minicomposites, J. Mech. Phys. Solid. 138 (2020), 103903.
[21] Zhengmao Yang, Junjie Yang, Investigation of long-term thermal aging-induced damage in oxide/oxide ceramic matrix composites, J. Eur. Ceram. Soc. 40 (4) (2020) 1549–1556.
[22] B. Moser, A. Rossoll, L. Weber, O. Beffort, A. Mortensen, Damage evolution of Nextel 610^{tm} alumina fibre reinforced aluminium, Acta Mater. 52 (3) (2004) 573–581.
[23] W.A. Curtin, B.K. Ahn, N. Takeda, Modeling brittle and tough stresscstrain behavior in unidirectional ceramic matrix composites, Acta Mater. 46 (10) (1998) 3409–3420.
[24] Jacques Lamon, Fiber Reinforced Ceramic Matrix Composites: A Probabilistic Micromechanics-Based Approach, Springer Singapore, Singapore, 2018, pp. 1–32.
[25] Zhengmao Yang, Yan Han, Multiscale modeling and failure analysis of an 8-harness satin woven composite, Compos. Struct. 242 (2020), 112186.